Towards a better description of cardiovascular function in pulmonary hypertension

Kind, T.

2012

document version
Publisher's PDF, also known as Version of record

Dynamic contrast-enhanced MRI for quantifying lung parenchymal blood perfusion

10

Evaluation of deconvolution methods

Taco Kind[1], Anton Vonk-Noordegraaf[1]
Barry Ruijter[2], J. Tim Marcus[2]

Departments of [1]Pulmonary Diseases, [2]Physics and Medical Technology, Institute for Cardiovascular Research, VU University Medical Center, Amsterdam, the Netherlands

Submitted

Abstract

Bolus-tracking dynamic contrast enhanced magnetic resonance imaging (DCE-MRI) is increasingly applied to quantify pulmonary perfusion. Quantification requires a deconvolution of a measured arterial input function (AIF) and tissue function (TIS) to obtain a residue function (R). From R pulmonary blood flow (PBF), pulmonary blood volume (PBV) and mean transit time (MTT) can be obtained. Deconvolution methods can be model-dependent or model-independent and generally differ in assumptions of the global shape of *R*, computational stability and oscillations in estimated *R*. It is unknown what deconvolution methods perform best for pulmonary perfusion quantification. Furthermore, it is unknown how delay and dispersion in estimated AIF affect perfusion parameters. This study evaluates the robustness of different deconvolution techniques and explores the role of delay and dispersion in pulmonary perfusion quantifications. All analyses were performed in control subjects, patients with pulmonary hypertension and patients with pulmonary atresia who underwent DCE-MRI. Results indicated that model-independent deconvolution using Tikhonov regularization with an optimized L-curve criterion and parameterization of *R* using B-splines was most robust and more robust than Tikhonov regularization alone. Delay correction of the contrast bolus arrival time was essential for accurate quantification, while dispersion had a negligible effect on perfusion estimates.

Keywords: dynamic contrast enhanced MRI ■ deconvolution ■ bolus delay and dispersion ■ pulmonary blood perfusion ■ residue function ■ delay

Introduction

ABSOLUTE QUANTIFICATION of blood perfusion using bolus-tracking dynamic contrast enhanced magnetic resonance imaging (DCE-MRI) is a useful technique in many applications. Perfusion parameters comprise pulmonary blood flow (PBF), pulmonary blood volume (PBV) and mean transit time (MTT).

Absolute quantification of perfusion parameters in the lung parenchyma is challenging for several reasons. First, the lungs consist of large gas-filled spaces with a relatively low percentage of lung parenchyma. This fact negatively affects the contrast-to-noise ratio (CNR). Second, the short transit time of blood in the lungs requires sufficiently high temporal resolution to measure the bolus passage with sufficient samples. Optimal perfusion quantification is thus a balance between temporal resolution and CNR[1]. Third, the level of inspiration during breath hold importantly determines computed pulmonary blood flow, with higher values at expiration[2].

The theoretical basis of perfusion quantification is the central volume principle[3], which assumes linear and stationary tissues. This implicates that the response of a tissue to an injected tracer is proportional with the dose, and that this response does not change during injection. The assumption of linearity is only true when an arterial input (i.e. arterial input function (AIF)) is measured directly at the inlet of a tissue. Since this is not possible in the lungs, the AIF is usually measured in the main pulmonary artery. This results in a delay and dispersion of the contrast bolus at the arrival in the lung parenchyma. Although these factors are usually disregarded in experimental settings it may lead to underestimation of blood flow[4,5].

The tissue concentration of contrast agent can be described as a convolution of the AIF with a residue function. This residue function is a tissue characteristic that fully defines tracer kinetics and thus the perfusion parameters. The residue function is defined as a positive, monotonically decaying function. It can be obtained from the AIF and the tissue concentration function with a deconvolution procedure. This tissue concentration function (or short tissue function) can be considered is an "output function" and is determined either in a part or in the whole tissue.[3] Since deconvolution is an ill-posed problem (i.e. perfusion parameters are sensitive to small perturbations of the data), the effect of inaccuracies in the measurements should be minimized. This is usually performed by application of constraints to the shape of the residue function that should be estimated. The groups of deconvolution methods can be classified as model-dependent and model-independent deconvolution methods. It is unknown how these methods differ from each other in estimating perfusion parameters. This knowledge is especially important when perfusion parameters need to be compared between patients, or when follow-up measurements are performed.

The aim of this study was twofold: 1) to explore the role of delay and dispersion on pulmonary perfusion parameters in experimental data of healthy control subjects and patients, and 2) to evaluate the robustness of several model-independent deconvolution techniques. All analyses were performed in control subjects and in different patient populations, including idiopathic pulmonary arterial hypertension (iPAH), chronic thromboembolic pulmonary hypertension (CTEPH) and pulmonary atresia patients (PA). Pulmonary parenchyma was detected by semi-automatic lung segmentation.

Methods

Patient data

All examinations were performed on a 1.5T Sonata MRI system equipped with a 6-element phased array coil, or a 1.5T Avanto MRI system equipped with a 32-element phased-aray coil (Siemens Medical Solutions, Erlangen, Germany). Using a 3-D gradient-echo sequence with parallel imaging, eight consecutive slices (each 15 mm thick) were obtained in the coronal plane during a 30-seconds end-inspiratory breath hold. MR parameters were: flip angle 25°, TR/TE 2.29-3.18/1.12 ms, matrix 320 × 150, acquired voxel size 2.3 x 1.3 x 15 mm

As soon as dynamic MR image acquisition was started, a Gadolineum-based contrast agent (Magnevist®; Schering, Berlin, Germany) was injected via an antecubital vein at a rate of 5 ml/s, followed by a 20-ml saline flush at the same rate. In all subjects, 0.2 ml/kg body weight of Magnevist^{R} was administered with a power injector.

Included in this study were data from 5 healthy controls subjects and 16 patients. Among the patients were 6 patients diagnosed with idiopathic pulmonary arterial hypertension (iPAH), 5 patients with pulmonary atresia (ATRESIA), and 5 patients with chronic thromboembolic pulmonary hypertension (CTEPH). PH was diagnosed according to a standard diagnostic workup. The diagnosis of pulmonary atresia was made in all patients on CT-angiography and pulmonary angiography. In these patients only the preserved lung was considered in the analysis. In all patients, invasive pressure measurements were performed.

Cardiac output was measured from main pulmonary artery flow acquired using phase-contrast velocity quantification. A 2- D spoiled gradient-echo pulse sequence was applied with an excitation angle of 15°, TR/TE 11/4.8 ms, matrix 208 x 256 and a receiver bandwidth of 170 Hz per pixel. Velocity sensitivity was initially set to 120 cm/s, but adjusted to lower or higher values in individual cases. Velocity encoding was interleaved resulting in a temporal resolution of 22 ms. Pulmonary flow was obtained using Medis Flow software package (Medis, Leiden, The Netherlands).

In iPAH patients, the mean pulmonary arterial pressure (mPAP) was 60 ± 7, resistance (PVR) 1259 ± 714 dyn × s × cm^{-5}, and CO 3.9 ± 1.5 L/min. In ATRESIA patients,

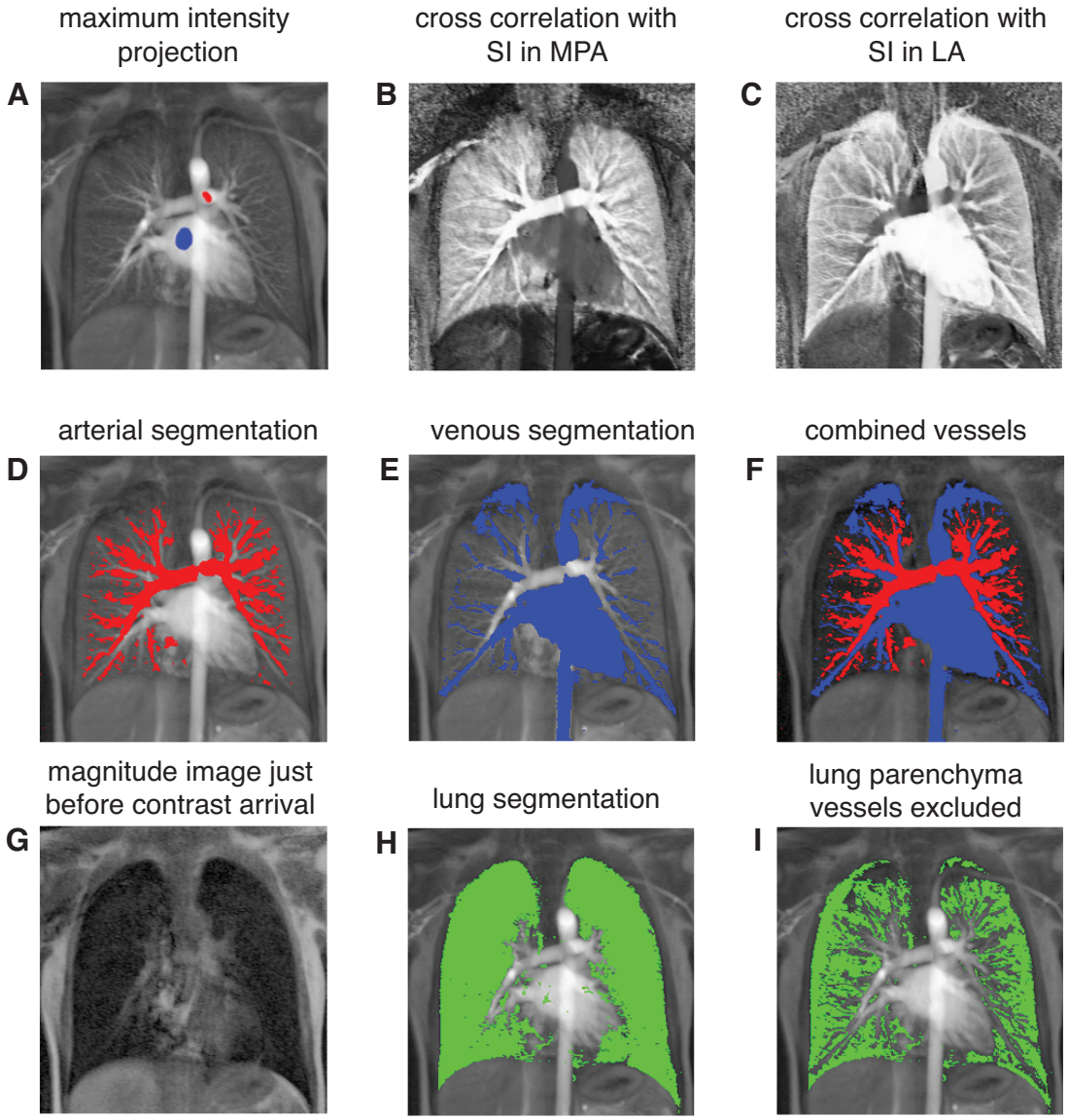

Figure 1 - Illustration of the semiautomatic lung parenchyma segmentation in a control subject in a mid thoracic slice; (*A*) Temporal maximum intensity projection that is used for selecting the MPA and LA SI functions from manually drawn regions of interest; (*B* and *C*) Standard cross-correlation of all pixels with the MPA and LV SI functions; (*D and E*) Segmentation of arteries and venes by selecting pixels with corresponding cross-correlation values above a pre-defined threshold value (see text). The selected pixels overlay the maximum intensity projection with arteries represented in red and venes in blue. Note that, the "venous" segmentation is not limited to pulmonary veins solely, but also includes parts of the systemic circulation; (*F*) Combined arteries and venes overlaying the maximum intensity projection; (*G*) Magnitude image just before the arrival of the contrast bolus, which is used for segmentation of the outer lung contours; (*H*) Segmentation of the lungs by selecting pixels in (*G*) with intensities below a pre-defined threshold value (see text), overlaying the maximum intensity projection; (*I*) Lung parenchyma obtained by excluding the vessels in (*F*) from the lungs in (*H*). MPA = main pulmonary artery; LV = left atrium; SI = signal intensity.

mPAP was 24 ± 18, PVR 367 ± 431 dyn × s × cm^{-5}, and CO 5.1 ± 1.4 L/min. In CTEPH patients, mPAP was 35 ± 21, PVR 1329 ± 1041 dyn × s × cm^{-5}, and CO 3.6 ± 1.9 l/min. In control subjects CO was 6.8 ± 1.7 L/min.

Semi-automatic lung segmentation

The lung parenchyma was segmented semi-automatically by segmentation of pulmonary arteries and veins[1,6,7], and of the outer lung contours. Subsequently, within the outer lung contours the segmented vessels were excluded in order to obtain the lung parenchyma. Pulmonary arteries were detected by standard cross-correlation between a signal Intensity (SI) function in the main pulmonary artery (determined from a manually drawn ROI in a central slice) and pixel SI functions[6] (Figure 1). With this approach a cross-correlation matrix was obtained with each pixels a value between -1 (negative correlation) and +1 (perfect correlation). Pixels with correlation values above a certain threshold were considered to belong to arteries and were rejected in the analysis of the lung parenchyma. On average a threshold of 0.7 was used, but this value was manually varied between 0.6 and 0.8 to exclude arteries to the same extent for every subject. This adjustment was based on visual inspection under the consideration that it is better to exclude too many than too few pixels. In the latter situation, a pixel corresponding to an artery would result in significant overestimation of parenchymal blood flow. To study the effect of leaving "arterial pixels" to the lung parenchyma, we also considered a threshold that was 0.1 higher than the threshold that was considered optimal. The obtained datasets were analysed separately.

To exclude venous vessels from the parenchyma, an SI curve was determined in the left atrium. Subsequently, this curve was cross-correlated with the pixel SI functions. Again a correlation matrix was obtained and pixels with correlation values above on average 0.7 (range 0.6 to 0.9) were excluded in the further analysis of the parenchyma (Figure 1).

In case of exuberant bronchial circulation, additional cross-correlation of pixel SI's with the aortic SI was performed, as pixel SI's in these vessels do not correlate well with the MPA or LA SI. Normally, bronchial vessels only supply nutrition to the parenchyma. However, in patients with CTEPH, the bronchial arteries are dilated resulting in increased flow[8]. These vessels become visible as a late phase of bolus passage.

To detect the outer border of the lung parenchyma an image was selected just before the tracer arrival and intensities were scaled between 0 and 1. Due to the air-filled spaces in the lungs, parenchymal intensity values are consistently lower than in the surrounding tissue. These pixels were selected using a threshold value between 0.1 and 0.15. Selected pixels that were outside the thorax were manually removed (Figure 1).

Theory

The central volume principle states that the transport of an injected tracer is linear and time-invariant. The response in a tissue $C_T(t)$ to an arbitrary arterial input function (AIF),

denoted as concentration curve $C_a(t)$ is then given by the convolution integral of this input with the residue function, $r(t)$.[9] Let $t \in \mathbb{Z}$ the discrete-time points with sequence $t = 0...N-1$, the discrete-time convolution yields:

$$C_T(t) = \Delta t \sum_{\tau=0}^{t} r(\tau) \cdot C_a(t-\tau) + \varepsilon(t), \text{ with } C_a(t) = 0 \text{ for } t < 0 \tag{1}$$

where Δt is the sampling interval and ε the signal noise.
For a more compact notation can be notated as

$$C_T = A \cdot r + \varepsilon \tag{2}$$

with

$$C_T = \begin{bmatrix} C_T(0) \\ \vdots \\ C_T(N-1) \end{bmatrix}, \quad r = \begin{bmatrix} r(0) \\ \vdots \\ r(N-1) \end{bmatrix}$$

and A a Toeplitz matrix, yielding

$$A = \Delta t \cdot \begin{bmatrix} C_a(0) & 0 & \cdots & 0 \\ C_a(2) & C_a(0) & \cdots & 0 \\ \vdots & \vdots & \ddots & 0 \\ C_a(N-1) & C_a(N-2) & \cdots & C_a(0) \end{bmatrix}, \quad A \in \mathbb{R}^{NxN}$$

The residue function r is assumed a monotonically decaying function with its initial amplitude a measure of pulmonary blood flow (PBF) in ml/100ml/min[9].

From the central volume principle, the relative pulmonary blood volume (PBV; in ml/100ml) can be derived by:

$$\text{PBV} = \frac{\int_0^\infty C_T(t)dt}{\int_0^\infty C_a(t)dt} \tag{3}$$

and mean transit time (MTT; in seconds) as:

$$\text{MTT} = \frac{\text{PBV}}{\text{PBF}} \cdot 60 \tag{4}$$

To compensate for discretization errors in matrix A, discretization was performed using the Volterra formula. This method was found to be most accurate compared to four other common discretization methods[10]. A can then be written as

$$\begin{cases} A_{i0} = A_i^- & \text{for } (0 < i \le n-1) \\ A_{ii} = A_0^+ & \text{for } (0 < i \le n-1) \\ A_{ij} = A_{i-j}^{\pm} & \text{for } (1 < i \le n-1,\ 0 < j < i) \\ A_{ij} = 0 & \text{elsewhere} \end{cases} \tag{5}$$

where $A_i^- = (2A_i + A_{i-1})/6$ and $A_i^+ = (2A_i + A_{i+1})/6$.

In principle, the residue function can be estimated by inversion of A. However, A is numerically ill conditioned and even small amounts of noise on the data may result in physiologically meaningless solutions. Therefore, this inversion should be regularized or the residue function should be parameterized to obtained stable solutions.

Regularization and parameterization

In a previous simulation study we evaluated several deconvolution methods to estimate PBF[11]. In the current study, some of the model-independent methods are applied to experimental DCE-MRI data obtained in the lungs. These methods are summarized below.

The inversion of (2) can be formulated as a linear problem:

$$\hat{r} = \arg\min \left\| C_T - Ar \right\|_2^2 \tag{6}$$

where $\hat{r}$ is the estimated residue function that can be obtained using a (generalized) singular value decomposition (SVD). To ensure that $\hat{r}$ is not too sensitive to perturbations the problem needs to be regularized. Several regularization methods are described below.

SVD truncation

The most often used (model-independent) technique in perfusion analysis and the simplest form of regularization is based on SVD of A with subsequent truncation of the smallest singular values[12]. The smallest singular values are due to noise and make unstable. Truncating these values results in an estimated residue function that is smoother than the unregularized solution. In this study, singular values were removed below 5% of the largest singular value to provide an optimal balance between stability and loss of information[11].

SVD with Tikhonov regularization

A drawback of SVD truncation is that it introduces unwanted oscillations in the time course of $\hat{r}$. An alternative is Tikhonov regularization, which provides a more gradual regularization without an abrupt cut-off for the singular values. This method is based on adding linear constraints to and has been shown on to improve the characterization of tissue residue functions[11,13]. The problem becomes:

$$\hat{r} = \arg\min\{\left\|C_T - Ar\right\|_2^2 + \lambda^2 \| Lr \|_2^2\}, \tag{7}$$

where L is a matrix operator and λ a weighting factor or regularization parameter. L should be chosen based on a priori information and the optimal λ should then be computed[14]. The solution is obtained using the generalized SVD. The simplest choice for L is the identity matrix, but is normally not appropriate to reduce oscillations in the solution vector. Other choices of L with increased regularization are the first or second derivative operator (defined as L = bidiag(*-1,1*) and L=tridiag(*1,-2,1*), respectively). A common method to derive the optimal value of λ is the L-curve criterion (LCC), which is based on the premise that the optimal value of λ is a compromise between the seminorm $\|Lr\|^2$ versus the residual norm $\|C_T - Ar\|^2$. A plot of these norms often reveals a characteristic L-shaped curve, with the assumption that the corner represents the point of optimal balance between both norms. For more detail of this method we refer to Hansen[14] and Calamante et al.[13]

SVD with TIkhonov regularization and B-splines parameterization

To further improve the stability of $\hat{r}$, the shape of the residue functions can be represented by using a basis of smooth B-splines[15,16]. The advantage of this parameterization is that it reduces the number of parameters that should be estimated. The residue function can be represented by[16]:

$$r(t) = \sum_{j=1}^{P} B_j^{(k)}(t) \cdot \alpha_j \tag{8}$$

where $B_j^{(k)}$ is the jth B-spline of order k for an equally distributed knot sequence containing P+k knots (equal distribution is not a requirement but would suffice and is also used in[16]), and α represents the real valued B-spline coefficients. In this study we used B-splines of order 4 and 5 break points[11].

The estimated tissue function can be expressed as:

$$\hat{C}_T(t,\theta) = \phi(t)^T \theta, \tag{9}$$

where

$$\theta = \begin{bmatrix} \alpha_1 \\ \vdots \\ \alpha_P \end{bmatrix}, \quad \phi(t) = \begin{bmatrix} B_1^{(k)}(t) \otimes C_T(t) \\ \vdots \\ B_P^{(k)}(t) \otimes C_T(t) \end{bmatrix}.$$

The problem in (6) is rewritten as:

$$\hat{\theta} = \arg\min \frac{1}{N} \sum_{t=0}^{N-1} \left\| C_T(t) - \hat{C}_T(t,\theta) \right\|_2^2, \tag{10}$$

where $\hat{\theta}$ is the optimal parameter vector that completely determines the estimated residue function. Inserting (9) in (10) yields:

$$\begin{aligned} \hat{\theta} &= \left[\frac{1}{N} \sum_{t=0}^{N-1} \phi(t) \phi^T(t) \right]^{-1} \frac{1}{N} \sum_{t=0}^{N-1} \phi(t) C_T(t) \\ &= \left[\frac{1}{N} \Phi \Phi^T \right]^{-1} \frac{1}{N} \Phi C_T(t). \end{aligned} \tag{11}$$

Because matrix $\Phi\Phi_T$ is ill-conditioned Tikhonov regularization is applied before inverting this matrix.

Conversion of signal intensity to tracer concentration

Concentration functions *C(t)* were approximated by enhanced SI functions[17]. Within certain limits, a linear relationship can be assumed between the vascular concentration and enhanced SI: *S(t)-S(0) = kC(t),* with S(t) the signal intensity as a function of time, and *k* a scaling factor that depends on the MR sequence (it is affected by e.g. flip angle and coil sensitivity) and may vary on voxel position space[17]. When it is assumed that *k* is independent of the tissue type, it is the same for input and tissue function, and thus cancels out in quantitative perfusion analysis. Before deconvolution, recirculation effects were removed by fitting a gamma-variate function to the SI functions[18], covering the time domain until signal intensity falls below 50% of the dynamic range. The fitted data were upsampled to a sample interval of 0.05s to avoid discretization errors (Figure 2).

Delay and dispersion

The fitted gamma-variate function was used to determine that bolus arrival time in the MPA and in the lung parenchyma. The parenchymal tissue function was shifted back in time to correct for the delay in bolus arrival. The presence of dispersion was evaluated by determining the peak time of estimated *r(t)*. A peak of *r(t)* at non-zero time would

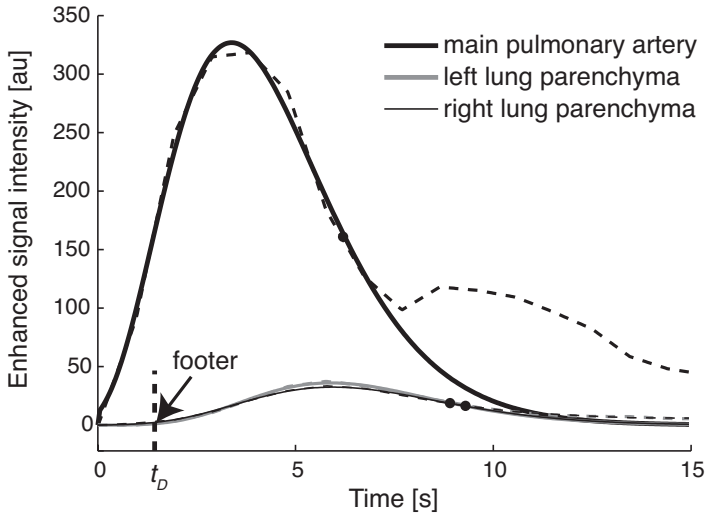

Figure 2 - Enhanced signal intensity functions determined in the same control subject as in Figure 1. Illustrated are signal intensity functions obtained in the main pulmonary artery, and in the left and right parenchymal lung tissue. Gamma-variate functions were used to fit the first pass of the contrast bolus in the three tissue regions, covering the time domain until signal intensity falls below 50% of the dynamic range (black dots). The footer of fitted gamma-variate functions in the left and right lung parenchyma represents the delay (t_D) relative to the contrast arrival in the main pulmonary artery.

indicate a delay and/or dispersion of the AIF at the inlet of the tissue[13]. When a tissue function is adequately corrected for a bolus delay, a peak of *r(t)* at non-zero time would then be solely due to dispersion of the AIF. To investigate the presence of dispersion, the B-spline + Tikhonov deconvolution was used to evaluate the peak of *r(t)* after adequate delay correction of the tissue function.

Statistics

Due to the absence of a Gaussian distribution all perfusion parameters are presented by median values and interquartile range. Parameters between controls and patients, and between the deconvolution methods, were compared using the Mann Whitney U test. A p-value < 0.05 was considered statistically significant.

Results

Lung segmentation

The segmentation of large vessels worked well in control subjects, but in patients occasionally problems occurred. As a result, optimal threshold values to differentiate between intrapulmonary vessels and lung parenchyma were found to be different than in control subject (0.7-0.9 versus 0.6-0.75). In these situations, additional manual adjustments were often required. Increasing the threshold by 0.1 to exclude less arterial pixels from the lung parenchyma resulted in an average overestimation of PBF of 28±16%, in PH patients,

Tabel 1 - Results of semiquantitative and quantitative perfusion analysis in controls subjects and in Patients.

	Control (N=5)	iPAH (N=7)	Atresia (N=5)	CTEPH (N=5)
Semiquantitative analysis				
Delay [s]	1.5 (1.0,2.0)	3.0 (2.0,3.4)*	1.5 (0.9,2.0)	1.9 (1.6,2.4)
S0 [au]	6.7 (5.9,6.9)	10.6 (8.5,14.3)*	7.3 (5.6,8.6)	6.9 (6.5,8.8)
PTT [s]	2.9 (2.5,3.3)	5.5 (5.1,6.7)*	3.4 (2.2,4.3)	3.9 (3.2,5.8)
SI max [au]	27.6 (25.2,38.8)	21.6 (20.6,30.4)	34.7 (27.0,39.4)	14.0 (7.1,27.0)
SI upslope [au/s]	8.5 (7.5,10.5)	3.1 (2.5,6.2)*	6.4 (3.9,10.4)	2.8 (1.5,6.1)
SI upslope [norm.]	0.3 (0.2,0.3)	0.2 (0.1,0.2)*	0.2 (0.2,0.3)	0.2 (0.2,0.3)
FWHM AIF [s]	6.1 (5.4,8.5)	12.5 (11.4,18.1)*	14.0 (8.8,14.8)	9.7 (9.3,14.1)*
FWHM tis [s]	8.0 (5.2,8.3)	9.5 (8.2,13.0)	9.2 (7.2,11.8)	5.5 (5.2,7.3)
FWHM ratio	1.0 (0.9,1.1)	0.7 (0.7,0.8)*	0.8 (0.7,0.9)	0.5 (0.5,0.6)*
Quantitative analysis				
B-splines + Tikhonov				
PBF [ml/100ml/min]	141.8 (119.7,151.8)	54.8 (45.6,58.8)*	114.2 (81.1,146.7)	43.4 (31.4,67.3)*
PBV [ml/100ml]	7.7 (7.4,9.3)	7.1 (6.4,8.4)	10.5 (9.1,18.1)	7.4 (4.4,12.1)
MTT [s]	5.3 (5.2,8.3)	14.2 (12.2,15.2)*	11.7 (8.1,12.9)	16.1 (8.7,24.4)
Tikhonov				
PBF [ml/100ml/min]	115.4 (82.9,190.6)	42.6 (36.0,57.4)*	171.1 (146.7,208.5)	34.2 (25.9,42.5)*
PBV [ml/100ml]	7.7 (7.3,9.3)	7.2 (6.4,8.3)	12.1 (9.0,19.6)	7.3 (4.4,12.4)
MTT [s]	7.8 (5.3,9.7)	16.4 (12.3,18.3)*	2.4 (0.5,8.1)	12.0 (5.1,21.7)
SVD truncation				
PBF [ml/100ml/min]	105.7 (88.6,137.2)	37.7 (34.6,48.7)*	85.0 (58.4,99.6)	34.2 (18.1,54.9)*
PBV [ml/100ml]	7.7 (7.3,9.3)	7.2 (6.4,8.3)	10.6 (8.9,18.3)	7.4 (4.4,12.1)
MTT [s]	7.2 (6.1,10.3)	18.8 (15.1,20.0)*	15.0 (13.0,17.5)*	21.8 (16.5,27.4)*

*Significantly different compared to control subjects ($p < 0.05$); comparisons were made using the Mann-Whitney U test. All data are median (interquartile range). Quantitative perfusion parameters are obtained from delay corrected enhanced signal intensity functions and are corrected for haematocrit (see methods). Data are obtained in left and right lung parenchyma separately and both are included in the analysis, except in pulmonary atresia patients in whom only data from the open lung is included. SI = signal intensity; S0 = baseline SI; PTT = peak transit time; SI max = maximum SI; SI upslope = maximum SI upslope; PBF = pulmonary blood flow; PBV = pulmonary blood volume; MTT = mean transit time. Normalized maximum SI upslope is obtained after normalizing the SI function for its maximum SI value.

while the average overestimation in the control subjects was 4±3%.

Exclusion of bronchial vessels in the CTEPH patients by using the aortic arch as arterial reference did not lead to improved segmentation of pulmonary vessels. Detection of the outer lung contours using a magnitude frame just before the contrast arrival worked fairly well in all subjects. The threshold values to select parenchymal pixels were adjusted between 0.1 and 0.15.

Semi-quantitative perfusion analysis

Table 1 shows the results of the semi-quantitative perfusion analysis. The results indicate that the delay in iPAH patients is significantly longer than in control subjects. Furthermore, the tissue signal intensity curves are broader, with a markedly increased PTT and FWHM, while their normalized SI-upslope is smaller than for controls. In the PA patients, no marked differences in semi-quantitative parameters are found compared to controls subjects. In CTEPH patients the delay is not significantly longer than in control subjects. Although the FWHM is increased, the PTT and normalized SI-upslope is not significantly different than in control subjects.

Quantitative perfusion analysis

Results of delay corrected quantitative perfusion analysis are also shown in Table 1. Figure 3 shows the results of absolute perfusion parameters obtained using B-spline + Tikhonov deconvolution. All methods yield decreased PBF values for iPAH and CTEPH patients, while a large range is observed in the Atresia patients. PBV was similar in iPAH and control subjects. For all methods the PBV was decreased in the CTEPH group. Although this decrease is not significantly different, the range is much larger than in control subjects. In iPAH and CTEPH patients, MTT values were increased with a large range in CTEPH patients, while in Atresia patients it was similar to control subjects.

The deconvolution methods differed significantly in accuracy and precision. The truncated SVD approach yielded significant oscillations in the estimated residue curve. In this study, the threshold value below which singular values were removed was 5% of the largest singular value. Decreasing this value to 4% lead to unstable solutions. Increasing this threshold lead to large oscillations with decreased values of PBF.

With Tikhonov deconvolution oscillations were significantly reduced. However, application of this technique resulted occasionally in unstable solutions of $r(t)$ when the L-curve criterion could not optimize the regularization parameter λ. This happened in five study subjects. Choosing L as a second order derivative operator could not stabilize these solutions, while parameterization of $r(t)$ by B-splines and subsequent Tikhonov regularization resulted in a more robust estimates of $r(t)$. Five break points were found optimal for stable and accurate estimates of $r(t)$.

Delay and dispersion

The effect of the delay as displayed in Table 1 on the absolute PBF is shown in Table 2. In all study subjects there was a considerable underestimation of PBF. The presence of dispersion was explored based on the peak time of $r(t)$. In all patients the peak of $r(t)$ occurred at $t = 0$s.

Tabel 2 - Differences between quantitative perfusion parameters obtained from delay corrected and from uncorrected parenchymal SI functions.

	Control (N=5)	iPAH (N=7)	Atresia (N=5)	CTEPH (N=5)
Quantitative analysis				
B-splines + Tikhonov				
Δ % PBF [ml/ml/min]	-50.3 (-56.0,-38.6)	-42.8 (-52.5,-40.0)	-49.2 (-53.5,-37.1)	-47.7 (-54.6,-25.8)
Tikhonov				
Δ % PBF [ml/ml/min]	-32.5 (-56.4,-20.6)	-30.7 (-86.5,-28.0)	-41.8 (-53.1,21.5)	-18.4 (-50.2,-14.1)
SVD truncation				
Δ % PBF [ml/ml/min]	-26.6 (-51.7,-22.7)	-54.1 (-72.3,-40.1)	-44.5 (-50.0,-37.0)	-52.4 (-66.1,-33.1)

All data are median (interquartile range). Abbreviations as in Table 1.

Discussion

In this study, different deconvolution methods to estimate pulmonary perfusion parameters were evaluated in healthy control subjects and in patients with idiopathic pulmonary hypertension (iPAH), chronic thromboembolic pulmonary hypertension (CTEPH) or pulmonary atresia (PA). Furthermore, the effects of delay and dispersion of the measured arterial input function (AIF) on pulmonary blood flow (PBF) were explored.

Lung segmentation

The advantage of the semi-automatic lung segmentation approach is a fast, less user-dependent approach, reducing potential overestimation of perfusion parameters by more accurate segmentation of lung parenchyma. Pulmonary arteries and veins were excluded by using double reference standard cross correlating all pixel SI's with the MPA and LA SI's[6,7]. A general drawback of the cross correlation method is the arbitrary cut-off value. This choice is always a trade-off between exclusion of vessels and preservation of lung parenchyma. Because there is a gradual decrease in vessel size distally from the pulmonary arteries (on a scale much smaller than the voxel size), perfusion parameters might decrease gradually by excluding more vessels[6].

Exclusion of bronchial vessels appeared inaccurate by using the aortic arch as arterial reference and was therefore manually excluded. Possibly, dispersion in the bronchial circulation might be underlying to this problem, as dispersed pixel SI functions do not correlate well with the non-dispersed aortic SI function.

The outer lung contour was segmented using a magnitude frame just before the arrival of the contrast bolus. Ingrisch et al.[1] suggested additional segmentation by calculating the normalized area under the curve (nAUC) of all pixel SI's (i.e. normalized by the AUC obtained in the MPA) and to exclude pixels with low values, assuming that these correspond

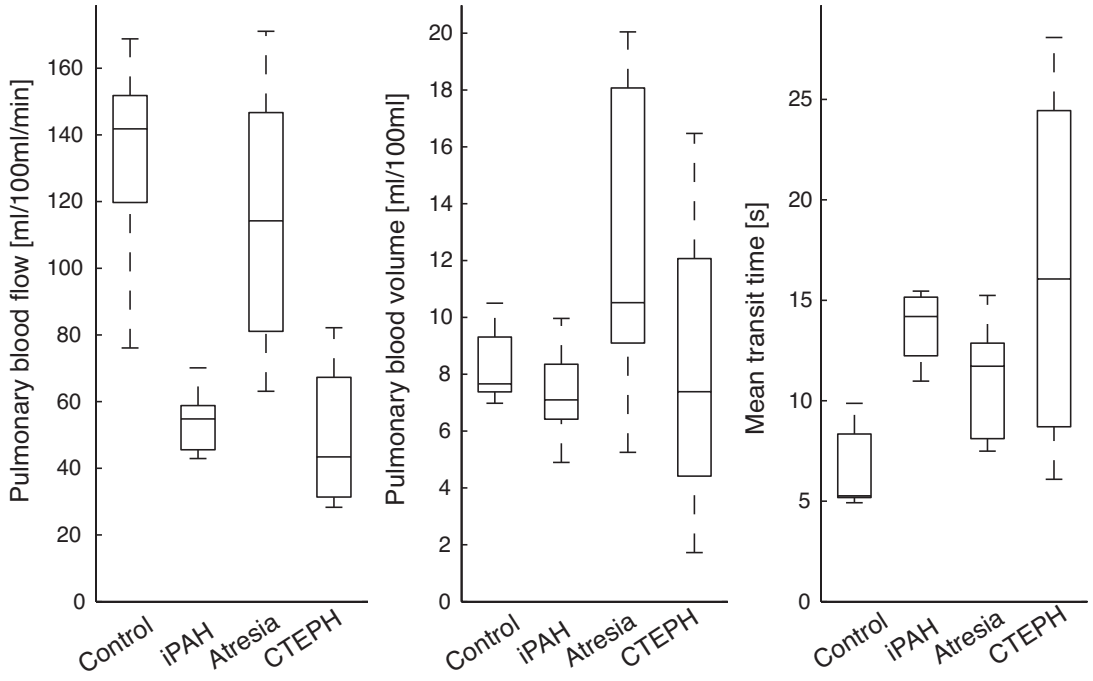

Figure 3 - Results of quantitative perfusion analysis using deconvolution with Tikhonov regularization and B-spline parameterization.

to noise. This approach worked fairly well in the control subjects in this study, but frequently failed in patients with lower mean signal intensity values in the lung parenchyma than in surrounding tissue.

Perfusion analysis

Since deconvolution is an ill-posed problem, constraints were applied to the estimation of the residue function *r(t)*, such as regularization or parameterization. Evaluation of the deconvolution techniques was based on volume-of-interest (VOI) perfusion analysis. Although regional perfusion defects cannot be detected using this approach, the CNR is substantially higher compared to pixel-based analysis, providing more accurate and precise results.

Delay and dispersion

Both in healthy control subjects and in patients a delay occurred, which was largest in iPAH patients. In pulmonary atresia patients no differences were found compared to control subjects, while in CTEPH patients a large range of delays was observed. Neglecting this delay resulted in large underestimation of PBF in all patients (Table 2). Since the delay differs between subjects, delay correction is especially important when comparisons are made between patients.

In this study the delay of bolus arrivals in the MPA and lung parenchyma was removed and subsequently Volterra discretization was performed. In VOI perfusion analysis, removing the delay prior to the deconvolution procedure is most accurate, but in case of pixel-by-pixel deconvolution this is more difficult since the delay may vary from pixel to pixel. In the latter situation, delay insensitive discretization methods should be considered (e.g. the block-circulant matrix[22] or the time-shift method[23]). These methods are a trade-off between delay invariance and absolute accuracy. Despite systemic errors, these methods should still be considered in pixel-based analysis[10].

In addition to a delay, the existence of dispersion of the contrast bolus may also result in errors in estimated perfusion parameters. In contrast to the delay, the dispersion is much more difficult to account for as it would require vascular models that are not known in advance[5]. Therefore, dispersion was detected by estimating the time of peak *r(t)*. Although this approach provides no quantification, at least, it provides information over the presence or absence of significant dispersion (assuming that the data is already delay corrected). Based on this method no dispersion was observed in all patients, suggesting limited effects of dispersion on global perfusion parameters. This might be explained by the short transit time in the pulmonary vasculature. This is in contrast to the much longer transit time in the brain. In particular in stroke patients considerable delays and dispersion may occur in the ipsilateral hemisphere[13].

Despite a residue function with its maximum at zero time, it does not totally exclude that regional dispersion exists. Especially, in CTEPH local stenosis or collateral flow may result in considerable delay and dispersion of local AIF's. This is, however, not included in the global AIF and may exaggerate any perfusion deficit[4]. On the other hand, a pixel-by-pixel deconvolution would require correction for delay and dispersion to avoid large estimation errors in perfusion defected regions. One solution would be to obtain local AIF's for each pixel. Willats et al.[24] proposed estimating these by using independent component analysis. In case absolute perfusion values are not of importance, a time-to-peak mapping, which reflect both delay and dispersion, are very useful for the identification of abnormal regions since delay and dispersion are additive.

Limitations

There are some limitations of the present study. First, all analyses were based on enhanced signal intensity curves. Therefore, factor *k* that relates signal intensity to concentration could not be estimated. In this study, a similar *k* in the AIF and tissue SI curve was assumed so that it cancels out in the quantitative analysis. However, it is unsure whether this assumption is correct in pulmonary perfusion quantification. This limitation could be circumvented using relative enhanced SI functions, but requires additional measurements of the pre-contrast relaxation rate (T1 mappings), which were not performed.

Second, perfusion quantification is limited by a maximum concentration of tracer agent in MPA to avoid T2* saturation effects and to maintain a linear association between observed signal intensity and tracer concentration[25]. The assumption of absence of saturation effects could not be warranted in this study.

Conclusion

Quantitative pulmonary perfusion analysis using DCE-MRI can be effective for assessment of perfusion in several pulmonary diseases. Model-independent deconvolution with parameterization of the residue function using B-splines and Tikhonov regularization was a robust technique for pulmonary perfusion quantification and was more robust than Tikhonov regularization alone. This technique has potential for more widespread application. Delay correction of the contrast bolus arrival time is required for accurate perfusion estimates. Dispersion of the contrast bolus has small effects on pulmonary perfusion estimates.

Acknowledgments

We are grateful to prof. F. Calamante (Brain Research Institute, Melbourne, Australia) for helpful discussions. We also acknowledge the use of the Regularization Tools for efficient implementation of the algorithms in this study. The Regularization Tools are available from NETLIB http://www.netlib.org.[26]

Sources of funding

T. Kind was financially supported by the Netherlands Organisation for Scientific Research (NWO), Toptalent grant, project number 021.001.120. A. Vonk-Noordegraaf was financially supported by the NWO, Vidi grant, project number 91.796.306.

References

1. Ingrisch, M., Dietrich, O., Attenberger, U. I., Nikolaou, K., Sourbron, S., Reiser, M. F., and Fink, C. Quantitative pulmonary perfusion magnetic resonance imaging: influence of temporal resolution and signal-to-noise ratio. *Invest Radiol.* 2010;45:7-14.
2. Fink, C., Ley, S., Risse, F., Eichinger, M., Zaporozhan, J., Buhmann, R., Puderbach, M., Plathow, C., and Kauczor, H. U. Effect of inspiratory and expiratory breathhold on pulmonary perfusion: assessment by pulmonary perfusion magnetic resonance imaging. *Invest Radiol.* 2005;40:72-79.
3. Meier, P., and Zierler, K. L. On the theory of the indicator-dilution method for measurement

of blood flow and volume. *J Appl Physiol.* 1954;6:731-744.

4. Calamante, F., Gadian, D. G., and Connelly, A. Delay and dispersion effects in dynamic susceptibility contrast MRI: simulations using singular value decomposition. *Magn Reson Med.* 2000;44:466-473.
5. Ostergaard, L., Chesler, D. A., Weisskoff, R. M., Sorensen, A. G., and Rosen, B. R. Modeling cerebral blood flow and flow heterogeneity from magnetic resonance residue data. *J Cereb Blood Flow Metab.* 1999;19:690-699.
6. Risse, F., Kuder, T. A., Kauczor, H. U., Semmler, W., and Fink, C. Suppression of pulmonary vasculature in lung perfusion MRI using correlation analysis. *Eur Radiol.* 2009;19:2569-2575.
7. Santini, F., Patil, S., Meckel, S., Scheffler, K., and Wetzel, S. G. Double-reference cross-correlation algorithm for separation of the arteries and veins from 3D MRA time series. *J Magn Reson Imaging.* 2008;28:646-654.
8. Ley, S., Kreitner, K. F., Morgenstern, I., Thelen, M., and Kauczor, H. U. Bronchopulmonary shunts in patients with chronic thromboembolic pulmonary hypertension: evaluation with helical CT and MR imaging. *AJR Am J Roentgenol.* 2002;179:1209-1215.
9. Zierler, K. Indicator dilution methods for measuring blood flow, volume, and other properties of biological systems: a brief history and memoir. *Ann Biomed Eng.* 2000;28:836-848.
10. Sourbron, S., Luypaert, R., Morhard, D., Seelos, K., Reiser, M., and Peller, M. Deconvolution of bolus-tracking data: a comparison of discretization methods. *Phys Med Biol.* 2007;52:6761-6778.
11. Kind, T., Houtzager, I., Faes, T. J., and Hofman, M. B. Evaluation of model-independent deconvolution techniques to estimate blood perfusion. *Conf Proc IEEE Eng Med Biol Soc.* 2010;1:2602-2607.
12. Ostergaard, L., Weisskoff, R. M., Chesler, D. A., Gyldensted, C., and Rosen, B. R. High resolution measurement of cerebral blood flow using intravascular tracer bolus passages. Part I: Mathematical approach and statistical analysis. *Magn Reson Med.* 1996;36:715-725.
13. Calamante, F., Gadian, D. G., and Connelly, A. Quantification of bolus-tracking MRI: Improved characterization of the tissue residue function using Tikhonov regularization. *Magn Reson Med.* 2003;50:1237-1247.
14. Hansen, P. C. Analysis of discrete ill-posed problems by means of the L-curve. *SIAM Review.* 1992;34:561-580.
15. Verotta, D. Estimation and model selection in constrained deconvolution. *Ann Biomed Eng.* 1993;21:605-620.
16. Jerosch-Herold, M., Swingen, C., and Seethamraju, R. T. Myocardial blood flow quantification with MRI by model-independent deconvolution. *Med Phys.* 2002;29:886-897.
17. Sourbron, S. Technical aspects of MR perfusion. *Eur J Radiol.* 2010;76:304-313.
18. Thompson, H. K. J., Starmer, C. F., Whalen, R. E., and Mcintosh, H. D. Indicator Transit Time Considered As a Gamma Variate. *Circ Res.* 1964;14:502-515.

19. Hansen, P. C. The L-curve and its use in the numerical treatment of inverse problems. *math.sintef.no.* 1999
20. Hanke, M. Limitations of the L-curve method in ill-posed problems. *BIT Numerical Mathematics.* 1996
21. Verotta, D. Two constrained deconvolution methods using spline functions. *J Pharmacokinet Biopharm.* 1993;21:609-636.
22. Wu, O., Ostergaard, L., Weisskoff, R. M., Benner, T., Rosen, B. R., and Sorensen, A. G. Tracer arrival timing-insensitive technique for estimating flow in MR perfusion-weighted imaging using singular value decomposition with a block-circulant deconvolution matrix. *Magn Reson Med.* 2003;50:164-174.
23. Smith, M. R., Lu, H., Trochet, S., and Frayne, R. Removing the effect of SVD algorithmic artifacts present in quantitative MR perfusion studies. *Magn Reson Med.* 2004;51:631-634.
24. Willats, L., Connelly, A., and Calamante, F. Improved deconvolution of perfusion MRI data in the presence of bolus delay and dispersion. *Magn Reson Med.* 2006;56:146-156.
25. Christian, T. F., Aletras, A. H., and Arai, A. E. Estimation of absolute myocardial blood flow during first-pass MR perfusion imaging using a dual-bolus injection technique: comparison to single-bolus injection method. *J Magn Reson Imaging.* 2008;27:1271-1277.
26. Hansen, P. C. Regularization tools version 4.0 for Matlab 7.3. *Numerical Algorithms.* 2007